PERGAMON

International Journal of Solids and Structures 39 (2002) 3289–3310

INTERNATIONAL JOURNAL OF SOLIDS and STRUCTURES

www.elsevier.com/locate/ijsolstr

Fast estimation of localized plasticity and damage by energetic methods

R. Desmorat *

Laboratoire de Modélisation et Mécanique des Structures, Université Paris 6, 8 rue du Capitaine Scott, F-75015 Paris, France

Received 19 July 2000; received in revised form 11 November 2001

Abstract

Structural failure often follows the initiation of cracks occurring at corners, free edges or interfaces. Continuum damage mechanics gives quantitative information about such cracking. But when used in a fully coupled manner (with elasticity and plasticity), it leads to costly computations.

In order to obtain helpful results for a fine and fast design, we propose to determine localized plasticity and damage by use of local post-calculations, which follow a simple elastic finite element computation. Energetic methods such as Neuber's, such as the strain energy density or as the complementary energy density methods, are justified for small scale yielding by use of path-independent integrals. They are extended to cyclic loading inducing fatigue and the case of thermal stresses is considered. For plane problems, these methods are completed by the analytical determination of the stress triaxiality along free edges or rigid inclusions.

The crack initiation conditions are then quickly estimated by the time-integration of Lemaitre's damage law. Calculations made for a holed plate (plane strain) and for a bi-axial testing specimen (plane stress) validate the methods.

Keywords: Neuber method; Plasticity; Damage; Crack initiation; Failure; Fatigue

1. Introduction

Many criteria are used for structural design and for material selection. Fracture mechanics is powerful when a cracking state exists. If the safety conditions are defined by the nonexistence of cracks, continuum damage mechanics (CDM) is the adequate design tool for structures submitted to monotonic loading as well as to fatigue loading (Lemaitre, 1971; Hayhurst and Leckie, 1973; Hult and Broberg, 1974; Murakami and Ohno, 1978; Lemaitre and Chaboche, 1985; Kracinovic and Fonseka, 1981; Lemaitre, 1992).

Damage may be taken into account in a fully coupled manner with elasticity and plasticity, but this leads to costly computations (Benallal et al., 1988; Grange et al., 2000) which are incompatible with an early

* Fax: +33-1-44-27-71-60.

E-mail address: desmorat@ccr.jussieu.fr (R. Desmorat).

0020-7683/02/$ - see front matter
PII: S0020-7683(02)00002-1

design and with repeated resolutions of the nonlinear mechanical problem. As pre-design is concerned, we need quick methods for the determination of structural failure, also in fatigue!

When small scale yielding conditions apply, we propose here a three-steps procedure based on an accurate linear elastic FE computation (first step) in which the layers are assumed to be elastic. The second step is the evaluation of the localized plasticity in the stress concentration zones previously exhibited. Local energetic methods such as Neuber's (1961), as the strain energy density (SED, Glinka, 1985) and the complementary energy density (CED) methods are justified by use of path-independent integrals (Section 2). Neuber's method is also completed for locally 2D problems by the study of the stress triaxiality along a free edge. The third step concerns the post-calculation of damage up to crack initiation by the time integration of Lemaitre's damage evolution law during the whole loading process.

2. Extended Neuber's method

Neuber's method initially proposed for shear (Neuber, 1961), looks like an energy equivalence between the elastic and the elasto-plastic calculations of the same geometry submitted to the same loading. For unidimensional states of stress, the product stress × strain in elasticity is assumed to be locally identical to the same product calculated by means of an elasto-plastic analysis. The plastic state is then determined as the matching of the constitutive equation with the hyperbola stress × strain = constant (Eq. (1), Fig. 4). This local method leads to a violation of the equilibrium. It is applied at stress concentration points.

2.1. Tridimensional states of stress

For tridimensional states of stress, the fundamental hypothesis may be written as

$$\sigma_{ij}\varepsilon_{ij} = (\sigma_{ij}\varepsilon_{ij})_{\text{elas}} \quad \text{monotonic loading} \tag{1}$$

$$\Delta\sigma_{ij}\Delta\varepsilon_{ij} = (\Delta\sigma_{ij}\Delta\varepsilon_{ij})_{\text{elas}} \quad \text{fatigue loading} \tag{2}$$

where $\Delta\sigma$ and $\Delta\varepsilon$ stand for the stress and strain amplitudes during a cyclic loading and $(\cdot)_{\text{elas}}$ means 'value determined from an elastic computation'. An alternative to Eq. (1) may be proposed as

$$\sigma_{\text{eq}}\varepsilon_{\text{eq}} = (\sigma_{\text{eq}}\varepsilon_{\text{eq}})_{\text{elas}} \tag{3}$$

where σ_{eq} and ε_{eq} are the von Mises equivalent stress and strain. The theoretical justification of Section 3 will lead us to use (1) instead of (3) as far as free edges are concerned.

Plastic behavior is described by an integrated Hencky–Mises law,

$$\sigma_{ij} = E_{ijkl}\varepsilon_{kl} - 3G\frac{\sigma^{\text{D}}_{ij}}{\sigma_{\text{eq}}}g(\sigma_{\text{eq}}) \tag{4}$$

$$p = g(\sigma_{\text{eq}}) = R^{-1}(\sigma_{\text{eq}} - \sigma_{\text{y}}) \tag{5}$$

where E_{ijkl} is the Hooke tensor (isotropic), E and G are the Young's and shear modulus, v the Poisson's ratio, p the accumulated plastic strain, $R(p)$ the isotropic hardening law and σ_{y} the yield stress. Eq. (5) corresponds to the yield criterion $f = \sigma_{\text{eq}} - R(p) - \sigma_{\text{y}} = 0$.

The von Mises equivalent stress is solution of the nonlinear equation (1) rewritten:

$$\frac{\sigma^2_{\text{eq}}}{3G} + g(\sigma_{\text{eq}})\sigma_{\text{eq}} = \frac{\Sigma^2_{\text{eq}}}{3G} + \frac{3(1-2v)}{E}\left[\Sigma^2_{\text{H}} - \sigma^2_{\text{H}}\right] \tag{6}$$

We note with capital letters the elastic solution $\Sigma_{ij} = (\sigma_{ij})_{\text{elas}}, \Sigma_{\text{eq}} = (\sigma_{\text{eq}})_{\text{elas}}, \Sigma_{\text{H}} = (\sigma_{\text{H}})_{\text{elas}}$.

The hydrostatic stresses of the elastic and plastic solutions (resp. Σ_{H} and σ_{H}) were assumed to be close in Lemaitre and Chaboche's (1985) work. In the general case they are different and can be derived from the knowledge of the stress triaxiality ratio Tr defined as the hydrostatic stress divided by the equivalent stress (Rice and Tracey, 1969),

$$\mathrm{Tr} = \frac{\sigma_{\mathrm{H}}}{\sigma_{\mathrm{eq}}} \quad \sigma_{\mathrm{H}} = \frac{\sigma_{kk}}{3} \tag{7}$$

The knowledge of this ratio is an important key in the application of Neuber's method. Introducing the triaxiality function R_v,

$$R_v = \tfrac{2}{3}(1+v) + 3(1-2v)\mathrm{Tr}^2 \tag{8}$$

Neuber's von Mises equivalent stress for 3D loading is finally solution of

$$\sigma_{ij}\varepsilon_{ij} = \frac{\sigma_{\mathrm{eq}}^2 R_v(\mathrm{Tr})}{E} + g(\sigma_{\mathrm{eq}})\sigma_{\mathrm{eq}} = \left(\sigma_{ij}\varepsilon_{ij}\right)_{\mathrm{elas}} = \frac{\Sigma_{\mathrm{eq}}^2 (R_v)_{\mathrm{elas}}}{E} \tag{9}$$

where $R_v(\mathrm{Tr})$ has to be determined.

2.2. Stress triaxiality ratio on free edges in plane problems

We expose here an original way to derive under plane deformation assumption the closed-form expression of the stress triaxiality for points located along free edges.

2.2.1. Plane stress

For a plane stress state, the points located along free edges are submitted to pure tension (or compression). The value of the triaxiality ratio is $\pm 1/3$.

2.2.2. Plane strain

For a plane strain state, one can show that Tr only depends on the accumulated plastic strain or, in an equivalent manner, only depends on the von Mises equivalent stress.

Elasticity: The triaxiality ratio evaluated at points located along free edges only depends on Poisson's ratio v. Tr neither depends on the loading type nor on its intensity. For $v = 0$, $\mathrm{Tr} = 1/3$ (some composite materials). For $v = 1/3$, $\mathrm{Tr} = 0.5$. For $v \approx 0.5$, $\mathrm{Tr} = 1/\sqrt{3} \approx 0.58$ (rubber). More generally,

$$\mathrm{Tr} = \frac{1+v}{3\sqrt{1-v+v^2}} \tag{10}$$

Plasticity with linear hardening: For plasticity with linear isotropic hardening, the yield function is written as $f = \sigma_{\mathrm{eq}} - Kp - \sigma_{\mathrm{y}} = 0$, where K is the plastic "tangent" modulus. The evolution laws governing the internal thermodynamics variables accumulated plastic strain p and plastic strains $\varepsilon_{ij}^{\mathrm{p}}$ are derived from the normality rule and from the consistency condition $\mathrm{d}f = 0$ during the plastic flow.

The boundary conditions (free edges of normal $\mathbf{e}_1$: $\sigma_{i1} = 0$), the plane strain condition $\varepsilon_{i3} = 0$ and the elasto-plastic behavior considered altogether lead to $(\dot{\sigma}_{33} - v\dot{\sigma}_{33})/E + (2\sigma_{33} - \sigma_{22})\dot{p}/2\sigma_{\mathrm{eq}} = 0$ and to the following set of equations:

$$\begin{cases} \sigma_{22} = u\sigma_{\mathrm{eq}} \quad \text{and} \quad \sigma_{33} = \frac{1}{2}\left(u - 2\sqrt{1 - \frac{3u^2}{4}}\right)\sigma_{\mathrm{eq}} \\ \frac{\mathrm{d}p}{Kp+\sigma_{\mathrm{y}}} = \dfrac{1 - 2v + \frac{3u}{2}\left(1 - \frac{3u^2}{4}\right)^{-1/2}}{2(K+E)\sqrt{1 - \frac{3u^2}{4}} - K(1-2v)u}\,\mathrm{d}u \end{cases} \tag{11}$$

with $\mathrm{d}\sigma_{\mathrm{eq}} = K\mathrm{d}p$ and where $u = \sigma_{22}/\sigma_{\mathrm{eq}}$ is a dead variable for the integration. No assumption about the loading proportionality is made. With the notations,

$$\chi = \frac{K(1-2\nu)}{2(K+E)} \qquad u_0 = \left(1-\nu+\nu^2\right)^{-1/2} \tag{12}$$

the closed-form expression for the $\mathrm{Tr}(p)$ law is then governed by the parametric representation:

$$\mathrm{Tr}(u) = \frac{u}{2} - \frac{1}{6}\sqrt{4-3u^2} \tag{13}$$

$$p(u) = \frac{\sigma_{\mathrm{y}}}{K}\left(\frac{\sqrt{1-\frac{3u_0^2}{4}}-\chi u_0}{\sqrt{1-\frac{3u^2}{4}}-\chi u}\right)^{\varpi} \exp\left(\mathscr{W}\left[\arcsin\left(\frac{\sqrt{3}u}{2}\right)\right]_{u_0}^{u}\right) - \frac{\sigma_{\mathrm{y}}}{K} \tag{14}$$

where

$$\mathscr{W} = \frac{2\sqrt{3}\chi}{3+4\chi^2}\left(1-\frac{2\chi}{1-2\nu}\right) \qquad \varpi = \frac{2\chi}{1-2\nu} + \frac{2\chi^2}{3+4\chi^2}\left(1-\frac{2\chi}{1-2\nu}\right) \tag{15}$$

Eqs. (13) and (14) may be rewritten as a law $\mathrm{Tr} = \mathrm{Tr}(p)$ or with Eq. (5) as $\mathrm{Tr} = \mathrm{Tr}(\sigma_{\mathrm{eq}})$: the triaxiality ratio on a free edge depends on the von Mises stress only (Fig. 1). For Poisson's ratios larger than 0.3, there

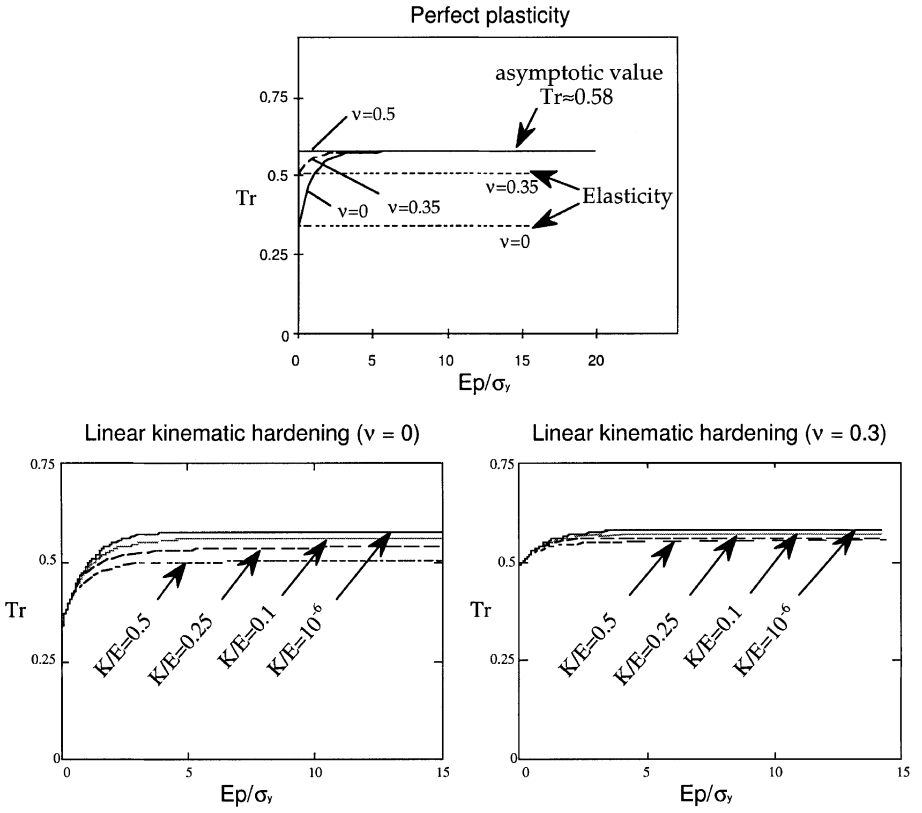

Fig. 1. Stress triaxiality along a free edge.

Table 1
Saturation value $\mathrm{Tr}_{\mathrm{sat}}$

	K/E			
	10^{-6}	0.1	0.25	0.5
$\mathrm{Tr}_{\mathrm{sat}}(\nu = 0)$	0.58	0.56	0.54	0.50
$\mathrm{Tr}_{\mathrm{sat}}(\nu = 0.3)$	0.58	0.57	0.56	0.55
$\mathrm{Tr}_{\mathrm{sat}}(\nu = 0.5)$	0.58	0.58	0.58	0.58

is a slight difference about Tr evaluated in elasticity or in plasticity: the triaxiality remains between 0.5 and 0.58. As soon as elastic strains are negligible, Tr reaches a saturation value. For metals it is $\mathrm{Tr} = 0.58$. The Table 1 gives the values of $\mathrm{Tr}_{\mathrm{sat}}$ as a function of K/E for $\nu = 0, 0.3, 0.5$.

Nonlinear hardening/damage: If the hardening law is not linear, variables p and u of Eq. (11) cannot be separated anymore. One has to fit a linear law in the plastic strain range under consideration and to apply Eqs. (13) and (14) as well. When isotropic damage occurs, the consideration of the effective stress concept (Kachanov (1958) and Section 4.1) formally leads to the same calculations and the determination of the triaxiality by Eqs. (13) and (14) remains valid.

To conclude, one can say that for standard Poisson's ratios and for plane deformation states, the stress triaxiality ratio at free edge points does not depend much on the loading, which is then quasi-proportional (stress tensor locally proportional to a constant tensor, see paragraph 2.2.2). For plane stress $\mathrm{Tr} = 1/3$ when for plane strain $\mathrm{Tr} = 0.58$ is a good value to consider for a quick method. In the general 3D case, Tr in plasticity may be taken equal to the stress triaxiality ratio computed in elasticity, $\mathrm{Tr} \approx (\mathrm{Tr})_{\mathrm{elas}}$. Once Tr is known, the triaxiality function R_v is easily calculated (Eqs. (8) and (9)) can be used to determine the von Mises equivalent stress as well as the accumulated plastic strain (Eq. (5)).

3. Theoretical justification and other energetic methods

A first attempt to justify Neuber's method is related to the virtual work principle. For any kinematically admissible displacement field $\mathbf{u}^*$ (structure Ω of frontier $\partial\Omega$),

$$\int_{\Omega} \sigma_{ij}\varepsilon^*_{ij}\,\mathrm{d}V = \int_{\partial\Omega} \sigma_{ij}n_j u^*_i\,\mathrm{d}S \tag{16}$$

If the small scale yielding hypothesis is made, one can compare the second member of (16) coming from an elastic and a plastic computation,

$$\left(\int_{\partial\Omega} \sigma_{ij}n_j u^*_i\,\mathrm{d}S\right)_{\substack{\text{elastic}\\ \text{computation}}} \approx \left(\int_{\partial\Omega} \sigma_{ij}n_j u^*_i\,\mathrm{d}S\right)_{\substack{\text{elasto-plastic}\\ \text{computation}}} \tag{17}$$

From the virtual work principle, we end up to a global but useless formulation of Neuber's Method:

$$\left(\int_{\Omega} \sigma_{ij}\varepsilon^*_{ij}\,\mathrm{d}V\right)_{\substack{\text{elastic}\\ \text{computation}}} \approx \left(\int_{\Omega} \sigma_{ij}\varepsilon^*_{ij}\,\mathrm{d}V\right)_{\substack{\text{elasto-plastic}\\ \text{computation}}} \tag{18}$$

Another way to proceed is to consider the path-independent integrals (Rice, 1968; Bui, 1978a)

$$\oint_C W\mathrm{d}y - \sigma_{ij}n_j\frac{\partial u_i}{\partial x}\mathrm{d}s \quad \text{and} \quad \oint_C W^*\mathrm{d}y - u_i n_j\frac{\partial \sigma_{ij}}{\partial x}\mathrm{d}s \tag{19}$$

vanishing on any closed contour which does not surround holes or cavities. W and W^* are respectively the SED and the CED from which the stresses and the strains are derived:

$$\sigma_{ij} = \frac{\partial W}{\partial \varepsilon_{ij}} \quad \varepsilon_{ij} = \frac{\partial W^*}{\partial \sigma_{ij}} \tag{20}$$

This framework applies to constitutive laws such as elasticity or as Hencky–Mises plasticity (no unloading). For incremental plasticity, the time-integration under proportional loading hypothesis leads to the appropriate definition of W or W^* (Eqs. (29)–(31), (35) and (36)).

3.1. Local energetic methods

Consider now stress concentration zones, confined as drawn in Figs. 2 and 3 and determined numerically first in elasticity then in elasto-plasticity. As long as small scale yielding applies, the sizes of the plastic zones given by the two analysis are not very different. For each computation, it is possible to evaluate integrals (19) along two open paths, C_1 along the free edge or the rigid inclusion (a rivet for example) and C_2 far from the plastic zone. Small scale yielding hypothesis equalizes the integrals along C_2 coming from the elastic and the elasto-plastic computations, i.e.,

$$\left(\int_{C_2} W \mathrm{d}y - \sigma_{ij} n_j \frac{\partial u_i}{\partial x} \mathrm{d}s \right)_{\substack{\text{elastic} \\ \text{computation}}} \approx \left(\int_{C_2} W \mathrm{d}y - \sigma_{ij} n_j \frac{\partial u_i}{\partial x} \mathrm{d}s \right)_{\substack{\text{elasto-plastic} \\ \text{computation}}} \tag{21}$$

By use of the path-independence property, these integrals are also equal along C_1. Along a free edge we get:

$$\left(\int_{C_1} W \mathrm{d}y \right)_{\substack{\text{elastic} \\ \text{computation}}} \approx \left(\int_{C_1} W \mathrm{d}y \right)_{\substack{\text{elasto-plastic} \\ \text{computation}}} \tag{22}$$

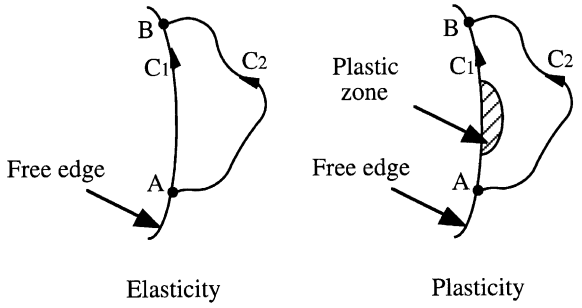

Fig. 2. Stress concentration zone close to a free edge.

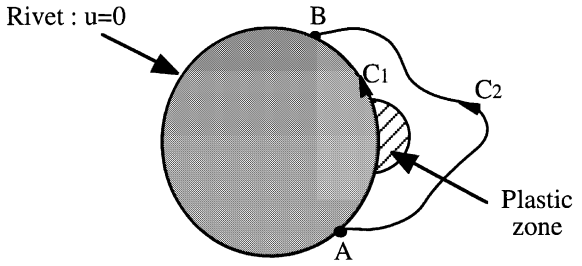

Fig. 3. Stress concentration zone close to a rigid inclusion.

By use of the dual integral,

$$\left(\int_{C_1} W^* \mathrm{d}y - u_i n_j \frac{\partial \sigma_{ij}}{\partial x} \mathrm{d}s\right)_{\substack{\text{elastic}\\ \text{computation}}} \approx \left(\int_{C_1} W^* \mathrm{d}y - u_i n_j \frac{\partial \sigma_{ij}}{\partial x} \mathrm{d}s\right)_{\substack{\text{elasto-plastic}\\ \text{computation}}} \tag{23}$$

which simplifies along a rigid inclusion ($\mathbf{u} = \mathbf{0}$) as:

$$\left(\int_{C_1} W^* \mathrm{d}y\right)_{\substack{\text{elastic}\\ \text{computation}}} \approx \left(\int_{C_1} W^* \mathrm{d}y\right)_{\substack{\text{elasto-plastic}\\ \text{computation}}} \tag{24}$$

Along a free edge stress concentration, the mean SED is locally the same for an elastic and for an elasto-plastic computations using the same boundary conditions (Eq. (22)). Along a rigid inclusion, the equality concerns the mean CED. For plastic zone with small gradient, we may write the local equality of the energies calculated in elasticity and in elasto-plasticity.

Because of the equality

$$\sigma_{ij}\varepsilon_{ij} = W + W^* \tag{25}$$

Neuber's method will give results (von Mises stress, accumulated plastic strain) between those given by the SED and CED methods.

To sum up, three energetic methods are justified for small scale yielding (as represented for tension in Fig. 4):

- Neuber's method (Eq. (1)),
- SED method: $W_{\text{plas}} = W_{\text{elas}}$,
- CED method: $W^*_{\text{plas}} = W^*_{\text{elas}}$.

In the following subsections we particularize these methods for elasto-plasticity with linear isotropic hardening and with exponential isotropic hardening (for monotonic proportional loading, kinematic hardening can be reduced to a supplementary isotropic contribution, Desmorat (2000)).

3.1.1. Linear isotropic hardening

Assume that an elastic computation has given the von Mises stress at stress concentration point, noted Σ_{eq}. The application of the energetic methods leads to the evaluation of the von Mises stress in plasticity. In general, the relationship $\sigma_{\text{eq}}(\Sigma_{\text{eq}})$ is implicit. Nevertheless, it can be explicited when linear hardening $R = Kp$ is considered.

For each method we define the auxiliary function h as the ratio (<1)

$$h(\Sigma_{\text{eq}}) = \frac{\sigma_{\text{eq}}}{\Sigma_{\text{eq}}} \tag{26}$$

The energetic methods are compared in Fig. 5 for tension triaxiality ($\mathrm{Tr} = 1/3$). For plastic materials with small K/E ratio (most materials), the complementary energy remains small in comparison with the strain energy. Neuber's and SED methods give then close results.

- 3D Neuber's method

$$\sigma_{ij}\varepsilon_{ij} = \frac{\sigma_{\text{eq}}^2 R_v}{E} + \sigma_{\text{eq}} g(\sigma_{\text{eq}}) = \frac{\sigma_{\text{eq}}^2 R_v}{E} + \frac{\sigma_{\text{eq}}(\sigma_{\text{eq}} - \sigma_{\text{y}})}{K} \tag{27}$$

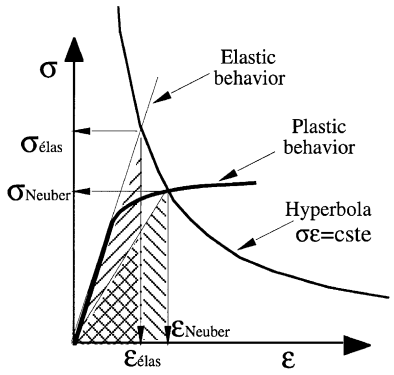

Neuber's method

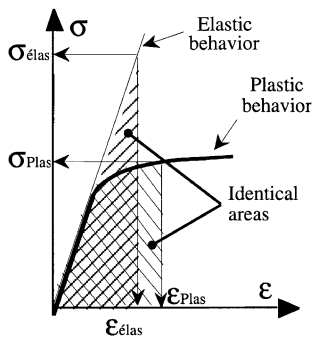

Strain Energy Density method (SED)

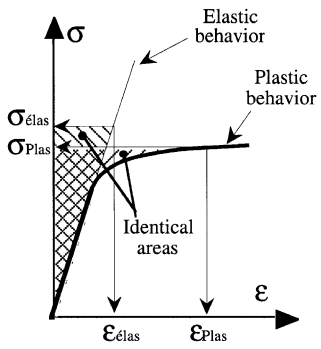

Complementairy Energy Density method (CED)

Fig. 4. Energetic methods (Neuber, SED, CED).

$$h(\Sigma_{\mathrm{eq}}) = \frac{\frac{E}{K}\sigma_{\mathrm{y}} + \sqrt{\left(\frac{E}{K}\sigma_{\mathrm{y}}\right)^2 + 4\left(R_v + \frac{E}{K}\right)\left(\Sigma_{\mathrm{eq}}^2 R_v\right)_{\mathrm{elas}}}}{2\left(R_v + \frac{E}{K}\right)\Sigma_{\mathrm{eq}}} \tag{28}$$

- 3D SED method

$$W = \frac{\sigma_{\mathrm{eq}}^2 R_v}{2E} + \int_{\sigma_{\mathrm{y}}}^{\sigma_{\mathrm{eq}}} \sigma_{\mathrm{eq}} g'(\sigma_{\mathrm{eq}})\,\mathrm{d}\sigma_{\mathrm{eq}} = \frac{\sigma_{\mathrm{eq}}^2 R_v}{2E} + \frac{\sigma_{\mathrm{eq}}^2 - \sigma_{\mathrm{y}}^2}{2K} \tag{29}$$

$$h(\Sigma_{\mathrm{eq}}) = \sqrt{\frac{\left(\Sigma_{\mathrm{eq}}^2 R_v\right)_{\mathrm{elas}} + \frac{E}{K}\sigma_{\mathrm{y}}^2}{\left(R_v + \frac{E}{K}\right)\Sigma_{\mathrm{eq}}^2}} \tag{30}$$

- 3D CED method

$$W^* = \frac{\sigma_{\mathrm{eq}}^2 R_v}{2E} + \int_{\sigma_{\mathrm{y}}}^{\sigma_{\mathrm{eq}}} g(\sigma_{\mathrm{eq}})\,\mathrm{d}\sigma_{\mathrm{eq}} = \frac{\sigma_{\mathrm{eq}}^2 R_v}{2E} + \frac{(\sigma_{\mathrm{eq}} - \sigma_{\mathrm{y}})^2}{2K} \tag{31}$$

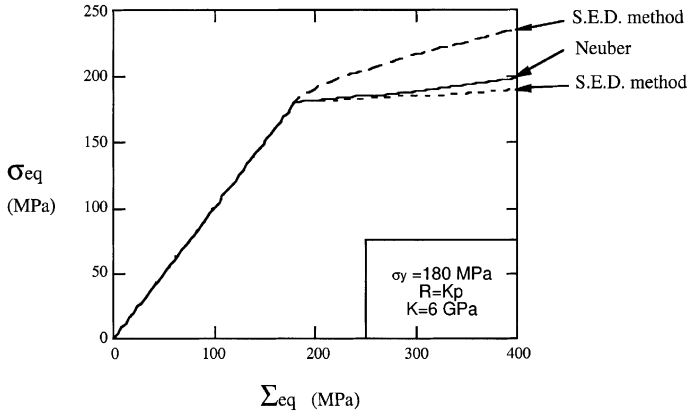

Fig. 5. Energetic methods for linear hardening; function $h(\Sigma_{\rm eq}) = \sigma_{\rm eq}/\Sigma_{\rm eq}$ ($E = 200$ GPa, $K = 6$ GPa, $\mathrm{Tr} = 1/3$).

$$h(\Sigma_{\rm eq}) = \frac{\frac{E}{K}\sigma_{\rm y} + \sqrt{R_v\left(\Sigma_{\rm eq}^2 R_v\right)_{\rm elas} + \frac{E}{K}\left[\left(\Sigma_{\rm eq}^2 R_v\right)_{\rm elas} - \sigma_{\rm y}^2 R_v\right]}}{\left(R_v + \frac{E}{K}\right)\Sigma_{\rm eq}} \tag{32}$$

3.1.2. Exponential isotropic hardening

Exponential hardening is written $R(p) = R_\infty(1 - \mathrm{e}^{-\gamma p})$ where R_∞ and γ are material parameters. The function g used in the calculation of the accumulated plastic strain (Eq. (4)) is then defined as:

$$p = g(\sigma_{\rm eq}) = -\frac{1}{\gamma}\ln\left(\frac{R_\infty + \sigma_{\rm y} - \sigma_{\rm eq}}{R_\infty}\right) \tag{33}$$

- Neuber's method

$$\sigma_{ij}\varepsilon_{ij} = \frac{\sigma_{\rm eq}^2 R_v}{E} + \sigma_{\rm eq} p = (\sigma_{ij}\varepsilon_{ij})_{\rm elas} \tag{34}$$

- SED method

$$W = \frac{\sigma_{\rm eq}^2 R_v}{2E} + \int_{\sigma_{\rm y}}^{\sigma_{\rm eq}} \sigma_{\rm eq}\,\mathrm{d}p = \frac{\sigma_{\rm eq}^2 R_v}{2E} + (R_\infty + \sigma_{\rm y})p - \frac{1}{\gamma}R(p) = W_{\rm elas} \tag{35}$$

- CED method

$$W^* = \frac{\sigma_{\rm eq}^2 R_v}{2E} + \int_{\sigma_{\rm y}}^{\sigma_{\rm eq}} p\,\mathrm{d}\sigma_{\rm eq} = \frac{\sigma_{\rm eq}^2 R_v}{2E} + (R(p) - R_\infty)p + \frac{1}{\gamma}R(p) = W^*_{\rm elas} \tag{36}$$

Again, the stress triaxiality in plasticity has to be known in order to apply the energetic methods, from which $\sigma_{\rm H} = \mathrm{Tr}\cdot\sigma_{\rm eq}$ and $\Sigma_{\rm H} = \mathrm{Tr}\cdot\Sigma_{\rm eq}$.

3.2. Extension to cyclic fatigue loading

Path-independent integrals (19) are still defined for cyclic loading. The only need is to consider a cyclic plasticity constitutive law written in terms of stress and strain amplitudes $\Delta\sigma_{ij}$, $\Delta\varepsilon_{ij}$. Formally,

$$\Delta\varepsilon_{ij} = \frac{\partial\omega^*}{\partial\Delta\sigma_{ij}} \quad \text{or} \quad \Delta\sigma_{ij} = \frac{\partial\omega}{\partial\Delta\varepsilon_{ij}} \tag{37}$$

where

$$\omega^* = \int_0^t \Delta\varepsilon_{ij}\frac{\mathrm{d}\Delta\sigma_{ij}}{\mathrm{d}t}\mathrm{d}t \quad \omega = \int_0^t \Delta\sigma_{ij}\frac{\mathrm{d}\Delta\varepsilon_{ij}}{\mathrm{d}t}\mathrm{d}t \tag{38}$$

3.2.1. Expression of the energetic methods

The following energetic methods extended to cyclic loading can be justified in the same manner than for the monotonic case:

$$\Delta\sigma_{ij}\Delta\varepsilon_{ij} = \left(\Delta\sigma_{ij}\Delta\varepsilon_{ij}\right)_{\text{elas}} \quad \text{extension of Neuber method} \tag{39}$$

$$\omega(\Delta\varepsilon_{ij}) = \omega_{\text{elas}} \quad \text{extension the SED method} \tag{40}$$

$$\omega^*(\Delta\sigma_{ij}) = \omega^*_{\text{elas}} \quad \text{extension of the CED method} \tag{41}$$

Still from an elastic computation, their application leads to the fast determination of the equivalent stress amplitude $(\Delta\underline{\sigma})_{\text{eq}}$ and of the accumulated plastic strain increment over one cycle Δp. If the applied load, noted F, ranges between two symmetric values $-F_{\max}$ and $+F_{\max}$, the knowledge of $(\Delta\underline{\sigma})_{\text{eq}}$ is sufficient to determine the maximum von Mises stress and the failure conditions (by integration of the damage law). If the loading is not symmetrical, the cyclic energetic method has to be completed by use of a monotonic method in order to evaluate the maximum von Mises stress. The corresponding damage law is derived in Section 4.3.

3.2.2. Potentials for linear kinematic hardening

For uniaxial tension–compression, the integration of the constitutive laws of elasto–plasticity with kinematic hardening leads to the following equations (with $\Delta\sigma$ stress amplitude, $\Delta\varepsilon$ strain amplitude, $\Delta\varepsilon^{\text{p}}$ plastic strain amplitude, Δp accumulated plastic strain increment over one cycle),

$$\Delta\varepsilon = \frac{2\sigma_{\text{y}}}{E} + \frac{\Delta\sigma - 2\sigma_{\text{y}}}{C_t} \tag{42}$$

$$\Delta p = 2\Delta\varepsilon^{\text{p}} = 2\frac{\Delta\sigma - 2\sigma_{\text{y}}}{C_t} \tag{43}$$

where C_t is the tangent modulus. The potentials needed to apply the energetic cyclic methods are:

$$\Delta\sigma\Delta\varepsilon = \left(\frac{2\sigma_{\text{y}}}{E} + \frac{\Delta\sigma - 2\sigma_{\text{y}}}{C_t}\right)\Delta\sigma \tag{44}$$

$$\omega = \frac{C_t}{2}\left[\Delta\varepsilon - 2\sigma_{\text{y}}\left(\frac{1}{E} - \frac{1}{C_t}\right)\right]^2 \tag{45}$$

$$\omega^* = \frac{C_t}{2}\left[\Delta\sigma + 2\sigma_{\text{y}}\left(\frac{1}{E} - \frac{1}{C_t}\right)\right]^2 \tag{46}$$

For general 3D cyclic loading, such potentials may be derived from the 3D constitutive laws under the assumption of a proportional loading: in any point M of the structure, the stress tensor remains proportional to a time-independent tensor $\underline{T} = \underline{T}(M)$. With the normalization $T_{\text{eq}} = \sqrt{\frac{3}{2}T^{\text{D}}_{ij}T^{\text{D}}_{ij}} = 1$, this leads to:

$$\underline{\sigma} = \underline{T}\mathrm{s}, \quad \mathrm{s} = \mathrm{s}(t) \quad \text{and} \quad |\mathrm{s}| = \sigma_{\mathrm{eq}} \tag{47}$$

$$\underline{X} = \underline{T}^{\mathrm{D}} X, \quad X = X(t) \tag{48}$$

$$\underline{\varepsilon}^{\mathrm{p}} = \tfrac{3}{2}\underline{T}^{\mathrm{D}}\varepsilon_{\mathrm{p}}, \quad \varepsilon_{\mathrm{p}} = \varepsilon_{\mathrm{p}}(t) \quad \text{and} \quad \dot{p} = |\dot{\underline{\varepsilon}}^{\mathrm{p}}| \tag{49}$$

and any 3D equation reduces to a scalar law. For example, the linear kinematic hardening evolution law $\underline{X} = 2/3C\underline{\varepsilon}^{\mathrm{p}}$ reduces to $X = C\varepsilon_{\mathrm{p}}$ with C the plastic modulus. The time-integration of the 3D constitutive equation is then similar to the one for tension/compression. We finally get the 3D laws as:

$$\Delta\varepsilon_{ij} = \frac{1+\nu}{E}\Delta\sigma_{ij} - \frac{\nu}{E}\Delta\sigma_{kk}\delta_{ij} + \Delta\varepsilon^{\mathrm{p}}_{ij} \tag{50}$$

$$\Delta\varepsilon^{\mathrm{p}}_{ij} = \frac{3}{2C}\frac{\Delta\sigma^{\mathrm{D}}_{ij}}{(\Delta\underline{\sigma})_{\mathrm{eq}}}\left\langle (\Delta\underline{\sigma})_{\mathrm{eq}} - 2\sigma_{\mathrm{y}}\right\rangle \tag{51}$$

$$\Delta p = 2\Delta\varepsilon^{\mathrm{p}} = \frac{2}{C}\left\langle (\Delta\underline{\sigma})_{\mathrm{eq}} - 2\sigma_{\mathrm{y}}\right\rangle \tag{52}$$

and Eqs. (42) and (43) are a particular case of (50) and (52).

The potentials are finally:

$$\Delta\sigma_{ij}\Delta\varepsilon_{ij} = \frac{(\Delta\underline{\sigma})^2_{\mathrm{eq}}R_v}{E} + \frac{(\Delta\underline{\sigma})_{\mathrm{eq}}}{C}\left\langle (\Delta\underline{\sigma})_{\mathrm{eq}} - 2\sigma_{\mathrm{y}}\right\rangle \tag{53}$$

$$\omega = \frac{(\Delta\underline{\sigma})^2_{\mathrm{eq}}R_v}{2E} + \frac{\left\langle (\Delta\underline{\sigma})^2_{\mathrm{eq}} - 4\sigma^2_{\mathrm{y}}\right\rangle}{2C} \tag{54}$$

$$\omega^* = \frac{(\Delta\underline{\sigma})^2_{\mathrm{eq}}R_v}{2E} + \frac{\left\langle (\Delta\underline{\sigma})_{\mathrm{eq}} - 2\sigma_{\mathrm{y}}\right\rangle^2}{2C} \tag{55}$$

where R_v is the triaxiality function (8) in which $\mathrm{Tr} = (\Delta\underline{\sigma})_{\mathrm{H}}/(\Delta\underline{\sigma})_{\mathrm{eq}}$, defines the cyclic stress triaxiality ratio (and $(\Delta\underline{\sigma})_{\mathrm{H}} = \text{trace}\ \Delta\underline{\sigma}/3$). Those equations are similar to Eqs. (27), (29) and (31) obtained for the monotonic case with linear hardening. They lead to the same closed from expressions $\Delta\sigma_{\mathrm{eq}} = h(\Delta\Sigma_{\mathrm{eq}})\Delta\Sigma_{\mathrm{eq}}$. The functions h are those of Section 3.1.1 in which σ_{eq}, Σ_{eq}, σ_{y} and K have to be formally replaced by $\Delta\sigma_{\mathrm{eq}}$, $\Delta\Sigma_{\mathrm{eq}}$, $2\sigma_{\mathrm{y}}$ and C.

3.3. Thermal stresses

Thermo-elasticity constitutive equation (56) defines an additional thermal expansion leading to thermal stresses,

$$\varepsilon_{ij} = E^{-1}_{ijkl}\sigma_{kl} + \alpha\theta\delta_{ij} \quad \text{or} \quad \sigma_{ij} = E_{ijkl}\varepsilon_{kl} - 3\alpha\kappa\theta\delta_{ij} \tag{56}$$

where θ is the temperature variation; $\alpha = \alpha(\theta)$ is the thermal expansion coefficient and κ is the compressibility modulus (elasticity coefficients may also depend on the temperature). The Helmhotz free energy density $\rho\psi$ and Gibbs free enthalpy $\rho\psi^*$ are classically:

$$\rho\psi = \tfrac{1}{2}E_{ijkl}\varepsilon_{ij}\varepsilon_{kl} - 3\alpha\kappa\theta\varepsilon_{kk} + \tfrac{1}{2}B\theta^2, \quad \rho\psi^* = \max_{\varepsilon}\left(\sigma_{ij}\varepsilon_{ij} - \rho\psi\right) \tag{57}$$

The derived state laws are:

$$\sigma_{ij} = \frac{\partial \rho\psi}{\partial \varepsilon_{ij}} \quad S_{\mathrm{v}} = -\frac{\partial \rho\psi}{\partial \theta} \tag{58}$$

or,

$$\varepsilon_{ij} = \frac{\partial \rho\psi^*}{\partial \sigma_{ij}} \quad S_{\mathrm{v}} = \frac{\partial \rho\psi^*}{\partial \theta} \tag{59}$$

S_{v} is the volumic entropy.

Extension of integrals (19) to thermo-elasticity introduces an additional term which is not a contour integral. Bui (1978b) proposes to write:

$$I = -\int_{\Gamma} \left\{ \rho\psi^* \,\mathrm{d}y - u_i n_j \frac{\partial \sigma_{ij}}{\partial x} \mathrm{d}s \right\} + \int_A S_{\mathrm{v}} \frac{\partial \theta}{\partial x} \,\mathrm{d}S \tag{60}$$

$$J = \int_{\Gamma} \left\{ \rho\psi \,\mathrm{d}y - \sigma_{ij} n_j \frac{\partial u_i}{\partial x} \mathrm{d}s \right\} + \int_A S_{\mathrm{v}} \frac{\partial \theta}{\partial x} \mathrm{d}S \tag{61}$$

The integrals thus defined are nevertheless path-independent and vanish for any closed path not surrounding holes or cavities. The area A is delimited by the contour Γ. When the material temperature is uniform, J reduce to Rice classical J-integral. An equivalent definition of J easier to use and called J_θ has been introduced by Aisworth et al. (1978),

$$J_\theta = \int_{\Gamma} \left\{ W \mathrm{d}y - \sigma_{ij} n_j \frac{\partial u_i}{\partial x} \,\mathrm{d}s \right\} + \int_A 3\alpha\kappa \frac{\partial \theta}{\partial x} \varepsilon_{kk} \mathrm{d}S \tag{62}$$

where the elastic energy is in fact $W = \rho\psi - B\theta^2/2$.

In the case of adiabatic conditions and in the case of a linear temperature variation, it is then possible to propose energetic methods by taking into account the temperature dependence of the material parameters. In the case of a general nonuniform temperature field, the existence of the additional surface integral leads to the nonequality of the energies locally calculated at a point in isothermal elasticity, in thermo-elasticity or in thermo–elasto-plasticity. Then, none of the energetic method may be justified.

3.3.1. Adiabatic conditions

An interesting case is to consider adiabatic loading conditions for which $S_{\mathrm{v}} = 0$. Eqs. (60) and (61) surface integrals vanish. Plasticity still being treated as nonlinear elasticity, Neuber's method remains unchanged when the SED method becomes the Helmhotz free energy density method,

$$\rho\psi = (\rho\psi)_{\text{thermo-elasticity}} \tag{63}$$

and the CED method becomes the Gibbs free enthalpy density method,

$$\rho\psi^* = (\rho\psi^*)_{\text{thermo-elasticity}} \tag{64}$$

3.3.2. Linear temperature variation

We consider here a loading (neither isotherm, neither adiabatic) with a linear temperature variation in the given zone of stress concentration. If θ is linear in the x_1-coordinate,

$$\theta = ax_1 + b \tag{65}$$

Bui (1978b) has shown that in this particular case the J_θ-integral can then be written as a contour integral,

$$J_\theta = \int_{\Gamma} \left\{ W(\varepsilon, \theta) n_1 + 3\alpha\kappa a (u_1 + g_2) n_1 - \sigma_{ij} n_j \frac{\partial u_i}{\partial x} \right\} \mathrm{d}s \tag{66}$$

where g_2 is a x_2-primitive of the ε_{22} strain component.

This last formula applies for elasto-plasticity as well with an adequate definition of W. The energetic methods proposed to evaluate edge-plasticity are then only justified when the second term inside integral (66) vanishes, i.e. for structures with a weak thickness temperature variation.

4. Localized damage and crack initiation conditions

We assume now that an elastic FE computation followed by a local energetic analysis gives a good estimation of the plasticity and the triaxiality at the stress concentration point. Crack initiation conditions are derived afterwards by use of CDM (post-processing). For a "fast" estimation of the damage, this uncoupled method gives results with the same order of accuracy than the energetic methods previously described.

For ductile damage and low cycle fatigue, damage occurs at the scale of the representative volume element (RVE) and Lemaitre's damage model applies. The damage evolution law is integrated straight forward with some simplifications.

We do not consider here the case of brittle damage or high cycle fatigue for which the behavior remains elastic at the RVE scale (plasticity and damage only occur at a micro-scale). The crack initiation conditions may nevertheless be determined by use of CDM with a two scale damage model (Lemaitre and Doghri, 1994; Lemaitre et al., 1999; Desmorat, 2000; Desmorat and Lemaitre, 2001).

4.1. Effective stress concept and damage law

Damage is described by the state variable D which models a loss of resisting area due to micro-cracks and micro-cavities ($0 \leqslant D < 1$). Failure of the RVE occurs when D reaches its critical value D_c. Isotropic damage is coupled to elasticity and plasticity by means of the effective stress tensor, $\tilde{\sigma}_{ij} = \sigma_{ij}/(1-D)$, i.e. the stresses σ_{ij} are replaced by $\tilde{\sigma}_{ij}$ in the elasticity law as well as in the yield criterion.

This feature is important because it means that the integrated plasticity law coupled to damage may be derived as the Hencky–Mises law in which the stress tensor is replaced by the effective stress tensor, i.e. $\tilde{\sigma}_{ij} = \partial W/\partial \varepsilon_{ij}$ (no unloading). Thus, when dealing with damage one has to consider the I and J contour integrals with σ_{ij} replaced by $\tilde{\sigma}_{ij}$. As long as plasticity and damage remain localized, the energetic methods are formally the same as before with σ_{ij} replaced by $\tilde{\sigma}_{ij}$. They directly lead to the fast estimation of the accumulated plastic strain and of the effective stress tensor.

The following damage evolution law (Lemaitre, 1992),

$$\dot{D} = \left(\frac{Y}{S}\right)^s \dot{p} \quad \text{if } p \geqslant p_D, \quad Y = \frac{\tilde{\sigma}_{eq}^2 R_v}{2E} \tag{67}$$

is used. It applies to damage induced by plasticity and takes into account the stress triaxiality effect on the growth of damage. The time integration of Eq. (67) allows for the quantification of D for monotonic loading, for fatigue loading (Dufailly and Lemaitre, 1995) as well as for creep fatigue conditions (Sermage et al., 2000). The damage strength S, the damage exponent s, the critical damage D_c are material parameters and p_D is the loading dependent damage threshold. The energy density release rate Y (associated with D) and the accumulated plastic strain p are state variables. Y is function of the effective stress (estimated by means of the energetic method) and of the triaxiality function R_v already defined (Eq. (8), R_v does not depend on the damage).

The damage threshold is considered here as related to the energy stored in the RVE during plastic loading (Desmorat, 2000; Lemaitre et al., 2000; Sermage et al., 2000). This allows to represent the very

different values experimentally obtained for monotonic and for cyclic loading: the damage threshold for pure tension, noted ε_{pD}, is of the order of magnitude of few percents (steels) when p_D in fatigue may reach few hundreds of percents. Based on the calculation of the energy stored in the RVE, the following relationship has been derived for fatigue:

$$p_D = \varepsilon_{pD}\left(\frac{\sigma_u - \sigma_y}{\sigma_{eq\ max} - \sigma_y}\right)^m \tag{68}$$

where the yield stress σ_y, the ultimate stress σ_u, the threshold in pure tension ε_{pD} and the exponent m are material parameters; $\sigma_{eq\ max}$ is the maximum von Mises stress reached over the cyclic loading.

The critical point of a structure is determined by means of the equivalent damage stress $\sigma^* = \sigma_{eq}R_v^{1/2}$ which takes into account the triaxiality effect when von Mises criterion does not. Crack initiation occurs at this point when D, given by the time-integration of Eq. (67), reaches its critical value:

$$D = D_c \rightarrow \text{crack initiation} \tag{69}$$

4.2. Unidimensional and threedimensional monotonic loading

Assuming that damage occurs once the hardening is saturated, the plasticity criterion is quasi-verified for the ultimate stress σ_u,

$$\frac{\sigma_{eq}}{1-D} - \sigma_u \approx 0 \tag{70}$$

Then Y is constant for proportional loading for which the triaxiality ratio Tr remains constant,

$$Y = \frac{\sigma_u^2 R_v}{2E} \tag{71}$$

An obvious integration of the damage law written for a threedimensional and for a onedimensional loading gives the accumulated plastic strain at crack initiation p_R as a function the stress traxiality, of the damage threshold ε_{pD} and of the strain at failure ε_R under uniaxial conditions,

$$p_R = \varepsilon_{pD} + \left(\varepsilon_R - \varepsilon_{pD}\right)R_v^{-s} \tag{72}$$

and the state of damage for any value of p simply is:

$$D = D_c\frac{p - \varepsilon_{pD}}{\varepsilon_R - \varepsilon_{pD}}R_v^s \tag{73}$$

In order to apply design criteria such as $N < N_R$ or $D < D_{given}$ the following quantities must be known:

- the values of the accumulated plastic strain p and of the triaxiality function R_v (from the structure calculation, energetic methods),
- as material parameters: the damage threshold ε_{pD}, the total strain at failure in pure tension ε_R, the critical damage D_c, the damage exponent s, the ultimate stress σ_u, the yield stress σ_y.

4.3. Low cycle fatigue

For low cycle fatigue, the damage D increases twice per cycle, each time corresponding to yield in tension (plastic strain increment δp_+, damage increment δD_+) and in compression (plastic strain increment δp_-, damage increment δD_-). We make here the hypothesis of a linear kinematic hardening.

If the fatigue loading consists in cycling between the same two loads $F_{\min}$ and $F_{\max}$, such an hypothesis leads to a closed stress–strain cycle and then to:

$$\delta p_+ = \delta p_- = \delta p = \frac{\Delta p}{2} \tag{74}$$

where Δp is the plastic strain increment over one cycle.

Further hypotheses are made in order to simplify the damage law for general cyclic loading. We assume first that the effective stress is correctly estimated from the previous local energetic analysis. The coupling of the energy release rate Y with damage is made by means of $\tilde{\sigma}_{\text{eq}}$ and Y is assumed not to vary much between the applied load inducing the reach of the yield stress and the maximum load $F_{\max}$ inducing the maximum von Mises stress $\sigma_{\text{eq max}}$, i.e.,

$$Y_+ \approx \frac{\tilde{\sigma}^2_{\text{eq max}} R_v}{2E} \tag{75}$$

Close to the minimum load $F_{\min}$ inducing the minimum von Mises stress $\sigma_{\text{eq min}}$, we get

$$Y_- \approx \frac{\tilde{\sigma}^2_{\text{eq min}} R_v}{2E} \tag{76}$$

From Eq. (67), the damage increment over one cycle N of loading is then

$$\begin{cases} \dfrac{\delta D}{\delta N} \approx \dfrac{\left(\tilde{\sigma}^{2s}_{\text{eq max}} + \tilde{\sigma}^{2s}_{\text{eq min}}\right) R_v^s}{2(2ES)^s} \Delta p & \text{if} \begin{cases} \Delta\sigma_{\text{eq}} > 2\sigma_{\text{y}} \\ p > p_{\text{D}} \end{cases} \\ \dfrac{\delta D}{\delta N} = 0 & \text{else} \end{cases} \tag{77}$$

The local maximum von Mises effective stress at the critical point $\tilde{\sigma}_{\text{eq max}}$ is determined by use of monotonic energetic methods, $\Delta\tilde{\sigma}_{\text{eq}}$ is the equivalent effective stress amplitude over the considered cycle and is determined by use of the cyclic methods. Then $\tilde{\sigma}_{\text{eq min}} = \tilde{\sigma}_{\text{eq max}} - \Delta\tilde{\sigma}_{\text{eq}}$.

For a complex history of loading, a numerical integration of Eq. (67) is necessary to obtain the number of cycles to crack initiation N_{R} corresponding to $D = D_{\text{c}}$ or the evolution of damage $D(N)$. If the loading is periodic then

$$D = \frac{\left(\tilde{\sigma}^{2s}_{\text{eq max}} + \tilde{\sigma}^{2s}_{\text{eq min}}\right) R_v^s \Delta p}{2(2ES)^s} (N - N_0) \tag{78}$$

where N_0 is the number of cycles to reach $p = p_{\text{D}}$ (p_{D} calculated by use of Eq. (68)),

$$N_0 = \frac{p_{\text{D}}}{\Delta p} \tag{79}$$

Finally,

$$N_{\text{R}} = N_0 + \frac{2(2ES)^s D_{\text{c}}}{\left(\tilde{\sigma}^{2s}_{\text{eq max}} + \tilde{\sigma}^{2s}_{\text{eq min}}\right) R_v^s \Delta p} \tag{80}$$

is the number of cycles to crack initiation. Eqs. (79)–(82) generalizes the so-called Manson–Coffin law (Coffin, 1954; Manson, 1959). For a single level loading, the amount of damage after N cycles is:

$$D = D_{\text{c}} \frac{N - N_0}{N_{\text{R}} - N_0} \tag{81}$$

If the loading is periodic by blocks, and if damage initiates during the first cyclic level after N_0 cycles,

$$\frac{N_1 - N_0}{N_{R1} - N_0} + \Sigma_{i>1} \frac{N_i}{N_{R_i}} = 1 \tag{82}$$

(if not please refer to Lemaitre and Desmorat (2001) and Desmorat and Lemaitre (2001)), The hypotheses stated induces the linear accumulation rule of Palmgreen–Miner only if N_0 is small ($N_0 \ll N_1$).

In order to apply design criteria such as $N < N_R$ or $D < D_{given}$ the following quantities must be known:

- the maximum and minimum effective von Mises stress $\tilde{\sigma}_{eq\ max}$ and $\tilde{\sigma}_{eq\ min}$, the value of the triaxiality function R_v and the accumulated plastic strain amplitude Δp (from the structure calculation, fast energetic methods),
- as material parameters: the Young's modulus E, the Poisson's ratio v, the yield stress σ_y, the ultimate stress σ_u, the plastic modulus C, the damage threshold in pure tension ε_{pD}, the exponent m, the critical damage D_c, the damage strength S, the damage exponent s.

4.4. Material properties of a 2 1/4 Cr steel

All the methods described need material parameters related to specific models. These parameters may be obtained from tensile tests either monotonic or cyclic at large strain amplitude. The properties of the 2 1/4 Cr steel used in headers of fossil plants are recalled here at room temperature. The full set of temperature dependent parameters (from 20 to 600 °C) as well as the identification procedure is given in (Sermage, 1998; Sermage et al., 2000).

4.4.1. Elasto-plasticity

From the tests results shown in Fig. 6 an exponential hardening describes well the plastic behavior. The material parameters for monotonic behavior at room temperature are: $E = 200$ GPa, $v = 0.3$, $\sigma_y = 180$ MPa, $R = R_\infty(1 - e^{-\gamma p})$, $R_\infty = 270$ MPa, $\gamma = 33$. The ultimate stress $\sigma_u = 450$ MPa is equal to $\sigma_y + R_\infty$.

For strains smaller than 4%, the hardening is considered as linear: $R = Kp$, $K = 6000$ MPa. For cyclic loading with strains smaller than 4%, linear kinematic hardening $\underline{X} = 2/3\ C\underline{\varepsilon}^p$ of modulus $C = K = 6000$ MPa is assumed.

4.4.2. Damage

The damage parameters are deduced from damage versus accumulated plastic strain curve, the damage being evaluated by its influence on the elasticity modulus. Monotonic (with unloading) and cyclic tests may be considered.

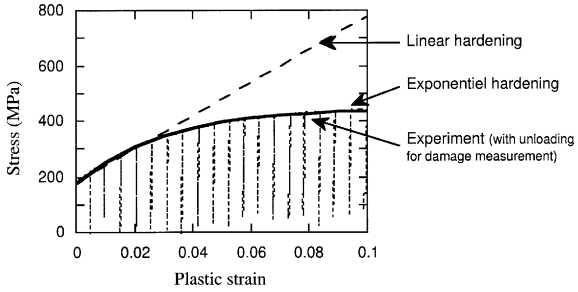

Fig. 6. Identification of plasticity parameters.

For the 2 1/4 Cr steel: $\varepsilon_{pD} = 0.12$, $m = 2$, $S = 2.8$ MPa, $s = 2$, $D_c = 0.2$ and the damage threshold in fatigue is given by Eq. (68).

5. Application to representative structures

5.1. Thick plate with a hole

Let us first consider the academic problem of a plate with a hole. The plate is large enough to be considered as infinite. It is thick enough for the plane strain conditions to apply. This last feature is important because previous works (Sharpe et al., 1992) have shown the limitations of classical Neuber method under such conditions. We will show that the stress triaxiality correction $\mathrm{Tr} = 0.58$ proposed in Section 1 makes the energetic methods (at least Neuber and SED) accurate under the plane strain assumption.

The closed-form elastic solution of the problem of an infinite plate with a hole submitted to a tensile remote stress σ_∞ seems to be due to Kirsh in 1898. It constitutes our elastic reference calculation with an usual elastic stress concentration factor of three.

For various loading intensity, we compare in Table 2 the fast plasticity estimations by the different methods at the stress concentration point (post-calculation of the analytical solution, Eqs. (34)–(36)) with an elasto-plastic FEM computation. The material considered is the 2 1/4 Cr steel at room temperature of Section 4.4.

At small plastic strains, small scale yielding occurs and SED method is the most accurate. This result is consistent with the theoretical justification of Section 3. As the applied load increases, the plasticity becomes less confined and Neuber method (with $\mathrm{Tr} = 0.58$) is the best.

5.2. Failure of a bi-axial specimen

A bi-axial testing specimen has been designed in order to exhibit stress concentrations and localized plasticity and damage at notches (Fig. 7). Computations of the specimen have been made in elasticity, in elasto-plasticity and in elasto-plasticity coupled to damage. Due to the load capacity of the machine, a 4.5 mm thin and 120 mm long specimen is considered and plane stress conditions apply. The edges are then in pure tension with a stress triaxiality ratio of 1/3.

For monotonic loading, the local plasticity levels are obtained by use of the energetic methods. They are compared to FE computations for points located on the edge (point A, Fig. 7) as well as for inside points (diagonal 0A).

A specimen also has been tested at room temperature in bi-axial fatigue on the LMT-Cachan tri-axial machine ASTREE, during a multi-level loading experiment (load driven experiment). The plasticity, damage and number of cycles to crack initiation are evaluated by use of the fast methods. This example of

Table 2
Comparison of the energetic methods

σ_∞ (MPa)	FE	Neuber	SED	CED
80	$\sigma_{eq\,max} = 181.5$ MPa $p = 2.5 \times 10^{-4}$	$\sigma_{eq\,max} = 184$ MPa $p = 6.5 \times 10^{-5}$	$\sigma_{eq\,max} = 182$ MPa $p = 3.4 \times 10^{-4}$	$\sigma_{eq\,max} = 202$ MPa $p = 3.7 \times 10^{-3}$
100	$\sigma_{eq\,max} = 187$ MPa $p = 1.22 \times 10^{-3}$	$\sigma_{eq\,max} = 188$ MPa $p = 1.4 \times 10^{-3}$	$\sigma_{eq\,max} = 184$ MPa $p = 7.7 \times 10^{-4}$	$\sigma_{eq\,max} = 216$ MPa $p = 6 \times 10^{-3}$
120	$\sigma_{eq\,max} = 193$ MPa $p = 2.1 \times 10^{-3}$	$\sigma_{eq\,max} = 194$ MPa $p = 2.4 \times 10^{-3}$	$\sigma_{eq\,max} = 188$ MPa $p = 1.3 \times 10^{-3}$	$\sigma_{eq\,max} = 228$ MPa $p = 8 \times 10^{-3}$

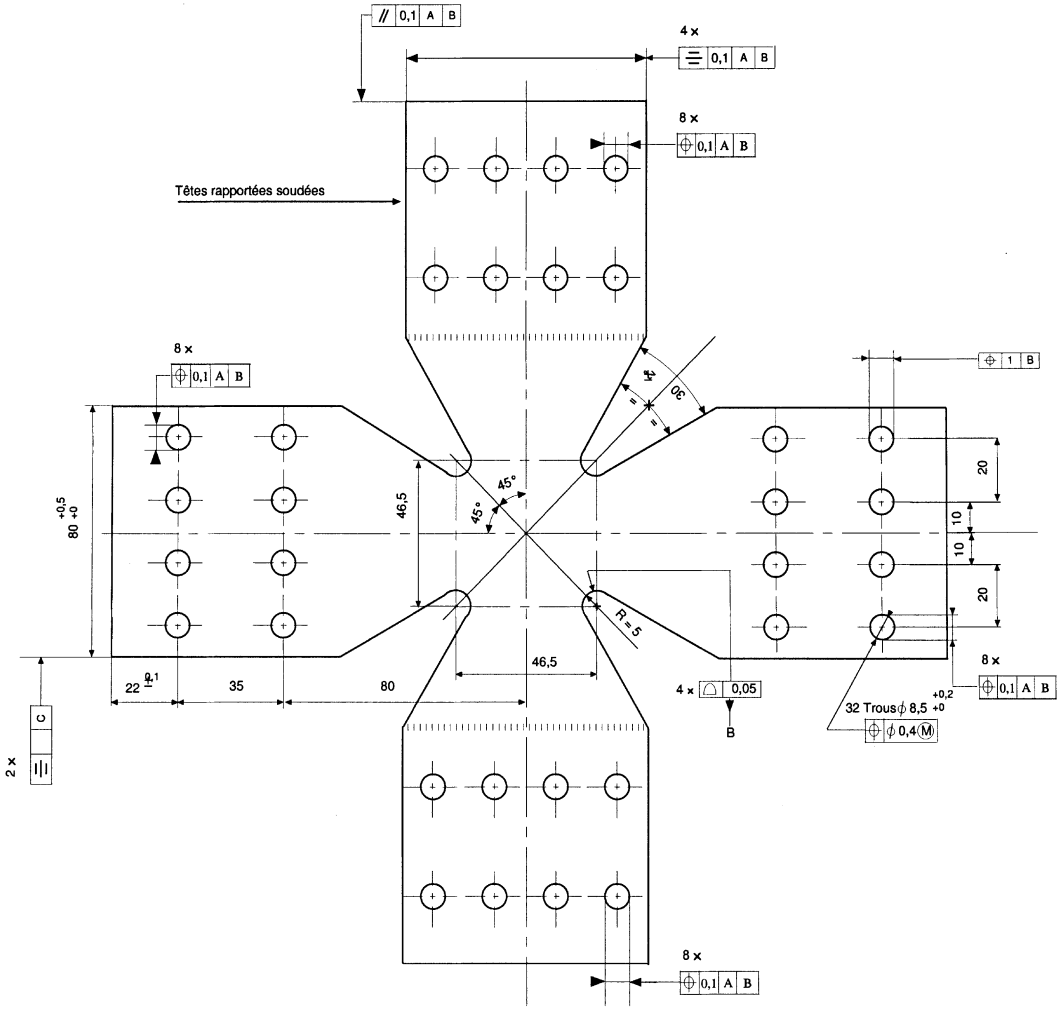

Fig. 7. Bi-axial testing specimen.

application is used here to validate the damage estimation up to failure (the damage is accumulated over each level up to $D = D_c$).

For information, note that five other specimens of the same material have been tested in creep and fatigue at variable temperature (up to 600 °C). The experimental results as well as a complete mechanical and numerical modeling can be found in (Sermage et al., 2000).

5.2.1. Monotonic loading

A symmetric displacement loading $U = 0.1$ or 0.5 mm is applied normally to each lateral side. Plasticity and damage are localized around the free edge point A for the first loading. For $U = 0.5$ mm, the sample is fully plastified.

The mesh of 1/4 of the sample is drawn in Fig. 8. In order to get accurate reference FE solutions it has been optimized by use of adaptative methods. Coorevits adaptative interface INTERF between ABAQUS and a mesh builder has been used (Coorevits et al., 1997).

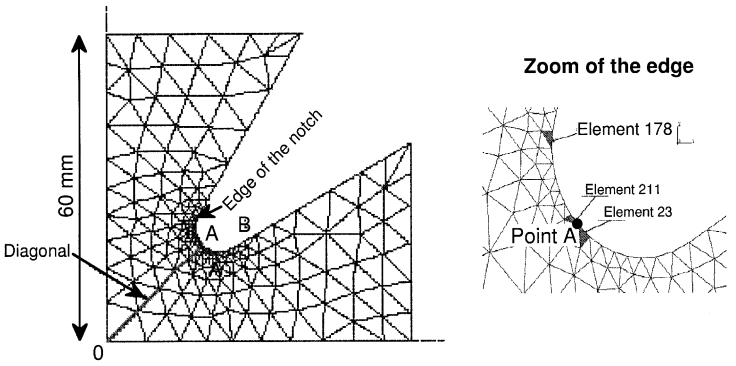

Fig. 8. Maltese cross specimen and optimized mesh (320 six nodes triangles).

ABAQUS elastic and plastic computation are presented. Fig. 9 represents the von Mises equivalent stress calculated along the diagonal line 0A (A: edge middle point) and Fig. 10 along the free edge AB. They also compare the different fast methods to a FE elasto-plastic FE computation. The elastic solution is used as an input to the plasticity evaluation by the local energetic methods (Eqs. (33)–(36)). The loading $U = 0.1$ mm corresponds to localized plasticity when $U = 0.5$ mm corresponds to a fully plastified sample. For $U = 0.5$ mm, the von Mises stress at the specimen center is $\Sigma_{eq} = 893.6$ MPa in elasticity and then $\sigma_{eq} = 240.6$ MPa in FE plasticity (to be compared to a 180 MPa yield stress).

The accuracy of Neuber and SED methods are of about a few percents when plasticity is localized (first loading) and of about 10% else: even if the methods have only been justified for small scale yielding, they still apply when it is no longer the case. Finally, SED method is a little bit better than Neuber's at free edge points, result coherent with Section 3 justifications.

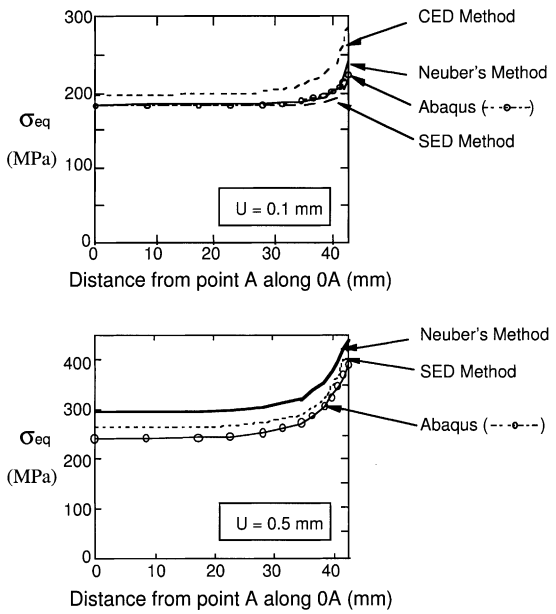

Fig. 9. von Mises stress along diagonal OA.

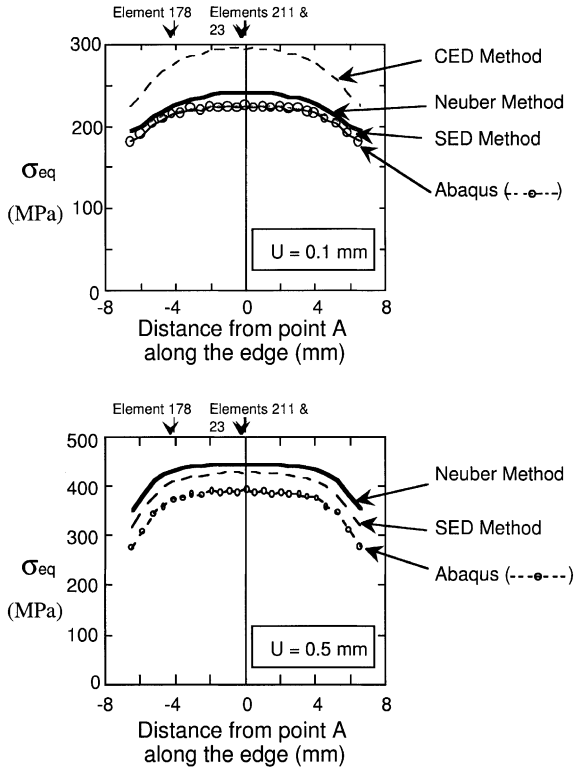

Fig. 10. von Mises stress along the edge AB.

5.2.2. *Multi-level fatigue loading*

As for the monotonic experiment, two in-phase proportional loads are applied on the lateral sides of the bi-axial specimen. The total loading consists in 13 blocks of cyclic loads varying between a zero minimum load and a constant maximum load $F_i^{\max}$ (Fig. 11). The first block is made of 38 000 cycles at $F_1^{\max} = 35$ kN, then the load is increased by 5 kN every 100 cycles up to $F_{13}^{\max} = 95$ kN. At this last level failure occurs after

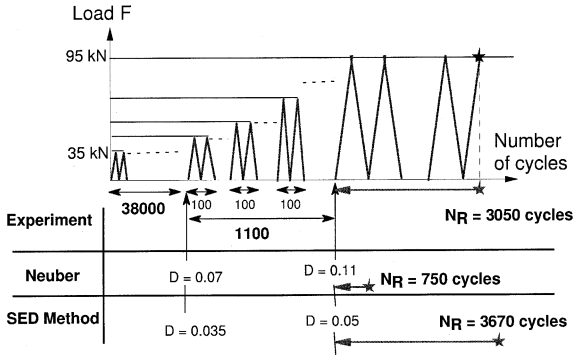

Fig. 11. Multi-level fatigue loading.

a number of cycles N_R^{95} (occurrence of a macroscopic crack in the edge). Experimentally a number $N_R^{95} = 3050$ cycles is measured (to be added to 39 100 for the total number of cycles to failure).

The minimum (zero) and maximum applied loads are not symmetric, then the monotonic as well as the cyclic form of the energetic methods need to be applied. Due to elasticity linearity, only one FE elastic computation is needed as reference.

Eqs. (26)–(30) give the maximum von Mises stress reached for each level when the cyclic methods of Section 2.2 (Eqs. (39), (40) and (52)–(54)) give the von Mises amplitude. The damage threshold in given by Eq. (68), it is reached after N_0 cycles (Eq. (81)). The accumulated plastic strain increment per cycle is calculated by use of Eqs. (43) or (52), the damage increment by use of Eq. (79). The damage increments over each block are summed up to $D = D_c$ which corresponds then to crack initiation.

At the beginning of the last level, $D = 0.11$ for Neuber method and $D = 0.05$ for SED method (Fig. 1) and finally a number of cycles at the last level $N_R^{95} = 750$ (Neuber) and $N_R^{95} = 3670$ (SED method) are estimated (to be compared to 3050).

The proposed procedure gives excellent results (at least for the SED method) after such a complex fatigue loading.

6. Conclusion

The energetic methods (Neuber, SED, CED) have been justified by means of path-independent integrals. They have been completed by the theoretical study of the stress triaxiality along a free edge (for plane problems). As far as tiaxiality is concerned to predict crack initiation, $Tr = 0.33$ for plane stress, $Tr = 0.58$ for plane strain and Tr equal to the triaxiality calculated in elasticity in the other cases are good candidates for correct approximations.

Damage Mechanics allows then for the estimation of the crack initiation conditions: accumulated plastic strain in ductile fracture, number of cycles in low cycle fatigue.

Two example of applications have been exposed:

- the academic problem of a holed plate (plane strain conditions),
- a bi-axial specimen (Maltese Cross shaped) tested in the triaxial testing machine ASTREE (plane stress conditions).

Both monotonic and fatigue loading have been applied. Numerical FE computations and experiments have been performed in order to evaluate the full procedure "application of an energetic methods followed by a damage analysis". The (corrected) Neuber method is often the best. The method of the SED seems better when used on a free edge with small plastic strains, as justified. The method of the CED would be better adapted to edges loaded by a rigid body. The difficulty would be then to determine the stress triaxiality along the interface.

To conclude, fast determination of localized plasticity and damage may be performed in early design of mechanical components for monotonic loading as well as for fatigue. The accuracy of the full procedure (application of an energetic methods followed by a damage analysis) seems sufficient for the design of mechanical components.

Acknowledgements

The author would like to thank S. Calloch and J.M. Virely for their help concerning the experiments made on the triaxial testing machine ASTREE of the LMT-Cachan.

References

Aisworth, R.A., Neale, B.K., Price, R.H., 1978. Fracture behavior in the presence of thermal strains. Proc. Inst. Mech. Engng. Conf. on Tolerance and Flaws in pressurized Components. London, pp. 171–178.

Benallal, A., Billardon, R., Doghri, I., 1988. An integration algorithm and the corresponding consistent tangent operator for fully coupled elastoplastic and damage equations. Comm. Appl. Numer. Meth. 4, 731–740.

Bui, H.D., 1978a. Dual path independent integral in the boundary-value problem of cracks. Engng. Fract. Mech. 6, 287–296.

Bui, H.D., 1978b. Mécanique de la rupture fragile. Masson.

Coffin, L.F., 1954. A study of the effects of cyclic thermal stresses in a ductile metal. Trans. ASME 76, 931.

Coorevits P., Dumeau, J.P., Pelle, J.P., 1997. Automatic generation of adapted meshes for design of three-dimensional structures, SMIRT, 14th International Conference on Structural Mechanics in Reactor Technology. pp. 17–24, Lyon.

Desmorat, R., 2000. Modélisation et estimation rapide de la plasticité et de l'endommagement, Mémoire d'habilitaion à diriger des recherches, Université Paris 6.

Desmorat, R., Lemaitre, J., 2001. Two scale damage model for quasi-brittle and fatigue damage. In: Lemaitre, J. (Ed.), Handbook of Materials Behavior Models, chapter Continuous Damage, Academic Press. Section 6.15, pp. 525–535.

Dufailly, J., Lemaitre, J., 1995. Modeling very low cycle fatigue. Dam. Mech., 4.

Grange, M., Besson, J., Andrieu, E., 2000. An anisotropic Gurson type model to represent the ductile rupture of hybrided Zircaloy-4 sheets. Int. J. Fract. 105, 273–293.

Glinka, G., 1985. Energy density approach to calculation of inelastic strain–stress near notches and cracks. Engng. Fract. Mech. 22, 405–508.

Hayhurst, D.R., Leckie, F.A., 1973. The effect of creep constitutive and damage relationships upon the rupture time of a solid circular torsion. J. Mech. Phys. Solids 21, 431–446.

Hult, J., Broberg, H., 1974. Creep rupture under cyclic loading. Proc. II Bulgarian National Congress of Theoretical and Applied Mechanics, Varna.

Kachanov, L.M., 1958. Time of rupture process under creep conditions, Izv. Akad NAUK. SSR.-Otd. Nauk. 8, 26–31.

Kracinovic, D., Fonseka, G.U., 1981. The continuous damage theory of brittle materials, Part 1 & 2. J. Appl. Mech., 809–824.

Lemaitre, J., 1971. Evaluation of dissipation and damage in metals submitted to dynamic loading. International Conference on Mechanical Behavior of Materials. The Society of Material Science, Kyoto, Japan.

Lemaitre, J., Chaboche, J.L., 1985. In: Mécanique des matériaux solides, Dunod, Paris. Mechanics of solid materials. Springer Verlag, Berlin, p. 1987.

Lemaitre, J., 1992. A course on damage mechanics. Springer Verlag, Berlin.

Lemaitre, J., Doghri, I., 1994. Damage 90: a post processor for crack initiation. Comp. Meth. Appl. Mech. Engng. 115, 197–232.

Lemaitre, J., Sermage, J.P., Desmorat, R., 1999. A two scale damage concept applied to fatigue. Int. J. Fract. 97, 67–81.

Lemaitre, J., Desmorat, R., Sauzay, M., 2000. Anisotropic damage law of evolution. Eur. J. Mech., A/Solids 19, 187–208.

Lemaitre, J., Desmorat, R., 2001. Isotropic and anisotropic damage law evolution. In: Lemaitre, J. (Ed.), Handbook of Materials Behavior Models, chapter Continuous Damage. Academic Press. Section 6.14, pp. 513–524.

Manson, S.S., 1959. Behavior of materials under condition of thermal stresses. NASA Tech. Note, 2933.

Murakami, S., Ohno, N., 1978. A constitutive equation of creep damage in pollicristalline metals. IUTAM Colloquium Euromech 111, Marienbad.

Neuber, H., 1961. Theory of stress concentration for shear strained prismatical bodies with an arbitrary non linear strain stress law. Trans. ASME 28, 540–550.

Rice, J.R., 1968. A path independent integral, the approximate analysis of strain concentration by notches, cracks. J. Appl. Mech. 35, 379–386.

Rice, J.R., Tracey, D.M., 1969. On the ductile enlargement of voids in triaxial stress fields. J. Mech. Phy. Sol. 17, 201–217.

Sermage, J.P., 1998. Fatigue thermique multiaxiale à température variable, Ph.D. Thesis Université Paris 6.

Sermage, J.P., Lemaitre, J., Desmorat, R., 2000. Multiaxial creep fatigue under anisothermal conditions. Fatigue Fract. Engng. Mater. Struct. 23 (3), 241–252.

Sharpe Jr., W.N., Yang, C.H., Tregoning, R.L., 1992. An evaluation of the Neuber and Glinka relations for monotonic loading. J. Appl. Mech. 92, S50–S56.